An Acad Bras Cienc (2023) 95(Suppl. 2): e20201533 DOI 10.1590/0001-3765202320201533
Anais da Academia Brasileira de Ciências | *Annals of the Brazilian Academy of Sciences*
Printed ISSN 0001-3765 I Online ISSN 1678-2690
www.scielo.br/aabc | www.fb.com/aabcjournal

GEOSCIENCES

Mangrove changes over the past decade in South and Southeast Brazil using spaceborne optical and SAR imagery

JOÃO PAULO N. LOPES, WILSON R. NASCIMENTO JR, CESAR G. DINIZ & PEDRO WALFIR M. SOUZA-FILHO

Abstract: Mangroves occur in the tropics and subtropics. This region is constantly covered by clouds and therefore highly challenging to map and monitor. Technological advances in remote sensing have increased the flexibility of performing such analyses. In this study, mapping and change detection were carried out for mangrove areas of the South and Southeast regions of Brazil between 2008 and 2016 using multisensor data and geographical object-based image analysis (GEOBIA). The 823.03 km² mangrove areas in study site in 2008 were reduced to 789.00 km² in 2016, representing a net loss of ~34 km². A change detection analysis of the mangrove areas showed a total gain of 138.21 km², a total loss of 172.24 km² and no change for 650.79 km². The GEOBIA classification accuracy was assessed by performing a statistical analysis of confusion matrix: (2008): global accuracy = 0.92, Kappa index = 0.84 and Tau index = 0.84; and (2016): global accuracy = 0.93, Kappa index = 0.86 and Tau index = 0.86. These results demonstrate the effectiveness of the GEOBIA to map and analyze mangrove dynamics. The results exhibit an excellent accuracy. Furthermore, mangrove areas in the south and southeast Brazil were mapped from the same methodological approach.

Key words: Landsat, JERS, ALOS PALSAR, GEOBIA, mangroves, change detection.

INTRODUCTION

Remote sensing is an important technique for the monitoring, quantification and detection of changes in mangroves. These ecosystems are coastal environments that are distributed worldwide in tropical and subtropical regions, and are highly impacted by anthropic actions, mainly housing expansion, agriculture and aquaculture activities (Glaser 2003, Alongi 2008).

Global mangrove area is estimated to be 137,760 km² for 118 countries, where 75% of the total area was concentrated in only 15 countries Giri et al. (2011). These data rank Brazil as having the third largest mangrove area of 9,940 km², behind Indonesia and Australia (Diniz et al. 2019). The mapping of mangroves in Brazil is constantly evolving. Initial studies involved visual interpretation of radar images (Terchunian et al. 1986, Herz 1991, Souza-Filho 2005), optical images and multi-sensor data fusion (Souza-Filho & Paradella 2002, Souza-Filho & Paradella 2005). The advent of computation enhanced automatic image classification and optimized the processing time of digital images. Several classification algorithms with specific capabilities were developed to aid visual analysis. The subsequent emergence of pixel value analysis (pixel-pixel classification) has provided more quantitative and replicable information than visual interpretation (Green et al. 1998).

Continuous advances in computational technologies and image segmentation tools that use geographic object-based image analysis (GEOBIA) have enabled extensive areas of the Earth's surface to be classified more rapidly than by a single image analyst (Kamal et al. 2015, Nascimento Jr et al. 2013). Using GEOBIA to map mangrove areas has increased methodological flexibility, precision, and statistical accuracy, while facilitating change detection analysis (Santos 2012, Nascimento Jr et al. 2013, Kamal et al. 2015, Pereira 2015).

In this study, GEOBIA was used to analyze different multisource remote sensing data (Landsat, ALOS PALSAR and digital elevation model) to map and detect changes in mangrove forests in the coastal areas of the South and Southeast regions of Brazil from 2008 to 2016.

MATERIALS AND METHODS

Study Area

The study area is located in South and Southeast Brazil and comprises a strip of five coastal states: Espírito Santo - ES, Rio de Janeiro - RJ, São Paulo - SP, Paraná - PR and Santa Catarina - SC (Figure 1). The highest demographic density of these states is located mainly in this regions (IBGE 2011), which may increase anthropic actions in areas near mangrove forests.

Remote sensor data set and digital image processing

The images used in this study include scenes from the satellite Landsat-5 TM (2008), Landsat-8 OLI (2016), ALOS-1 PALSAR (2008) and ALOS-2 PALSAR (2016). In addition, digital elevation models - DEM (Kartikeyan et al. 1998) were

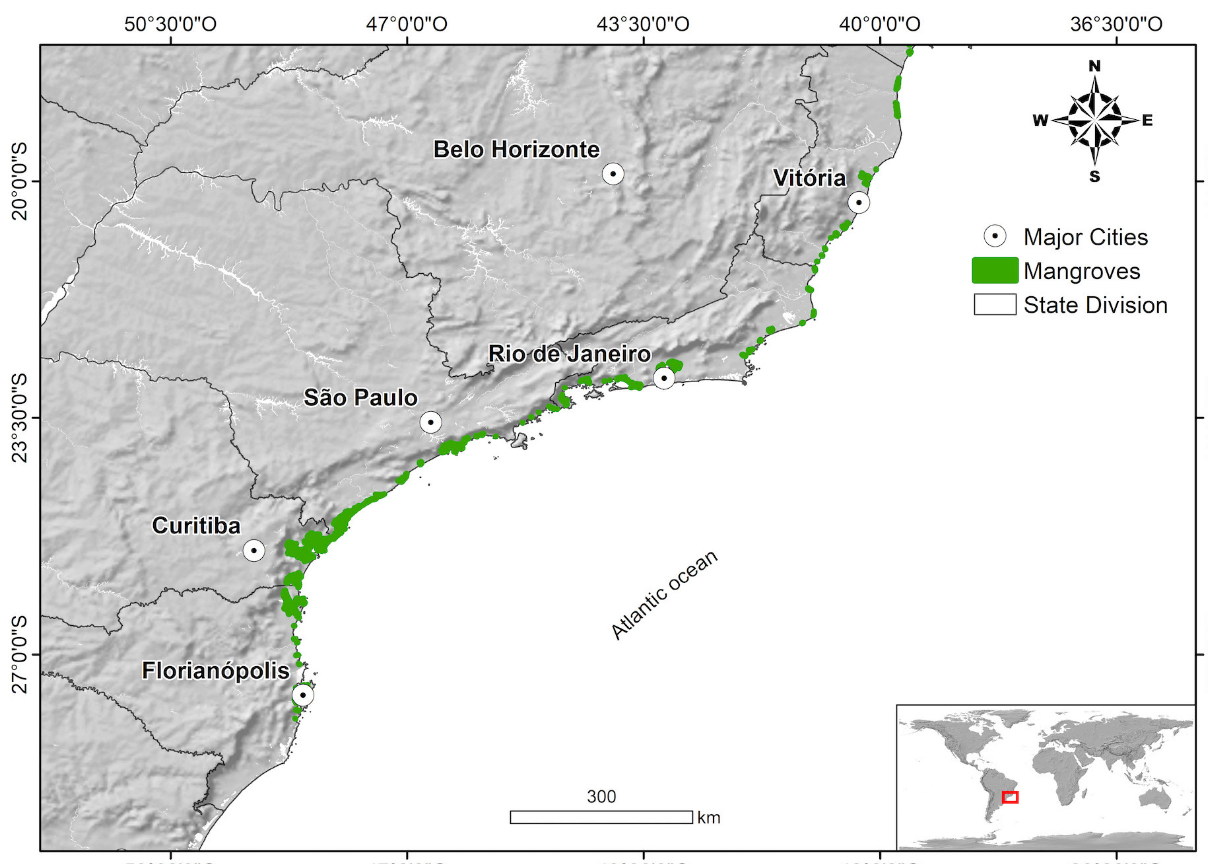

Figure 1. Distribution map of mangroves for coastal states in South and Southeast Brazil

acquired from the Shuttle Radar Topography Mission – SRTM in 2000 and from ALOS PALSAR in 2016. Table I shows the main characteristics of the data used.

The Landsat satellite images and the SRTM DEMs were obtained from the “Earth Explorer” portal managed by the United States Geological Survey – USGS (https://earthexplorer.usgs.gov), whose data characteristics and pre-processing steps are described in USGS (2012). The ALOS PALSAR images were acquired through the Japan Aerospace Exploration Agency – JAXA website (https://jda.jaxa.jp/en/). It is a fully polarimetric instrument, which operates in L-band, with 23.6 cm in wavelength (Rosenqvist et al. 2007). Figure 2 shows an example of a set of images used to map the mangrove regions in the study area.

An atmospheric correction was performed on the optical images to reduce the effects of atmospheric brightness in the scenes. Each digital number was converted to ground reflectance using the atmospheric correction module (ATCOOR) of PCI Geomatica software (2017).

The ALOS PALSAR images were pre-processed using Envi 5.5 software. The images were reprojected to WGS84 datum, mosaiced and finally converted to backscatter using eCognition Developer software v. 9.

Object-oriented classification and segmentation

This study was developed from geographical object-based image analysis. The remote sensing images were segmented at different levels using the same scale and heterogeneity parameters. However, different weights were assigned to each band/sensor to explore the qualities of different images for certain specific functions.

Next, an unsupervised classification algorithm was used to obtain three main classes

Table I. Main characteristics of remote sensing data.

Satellite/sensor	Type	Bands length/strip	Polarization	Resolution
ALOS/PALSAR	SAR	L (23.5 cm)	HV	10 m
ALOS/PALSAR DEM	SAR	L (23.5 cm)	-	30 m
SRTM DEM	SAR	C (5.6 to 7.5 cm)	-	30 m
Landsat 5 - TM	Optical	B1 (0.45 - 0.52 µm) B2 (0.52 - 0.60 µm) B3 (0.63 - 0.69 µm) B4 (0.76 - 0.90 µm) B5 (1.55 - 1.75 µm)	-	30 m
		B6 (10.4 - 12.5 µm)		120 m
		B7 (2.08 - 2.35 µm)		30 m
Landsat 8 - OLI	Optical	B1 (0.43 - 0.45 µm) B2 (0.45 - 0.51 µm) B3 (0.53 - 0.59 µm) B4 (0.64 - 0.67 µm) B5 (0.85 - 0.88 µm) B6 (1.57 - 1.65 µm) B7(2.11 - 2.29 µm)	-	30 m
		B8 (0.50 - 0.68 µm)		15 m
		B9 (1.36 - 1.38 µm)		30 m

(water bodies, upland, and mangrove) and two secondary classes (cloud and mangrove below cloud). To better define the coastline of the study area, the radar images in segmentation level 1 were assigned higher weights than other image types, because radar images are not subject to interference from clouds and are therefore more reliable.

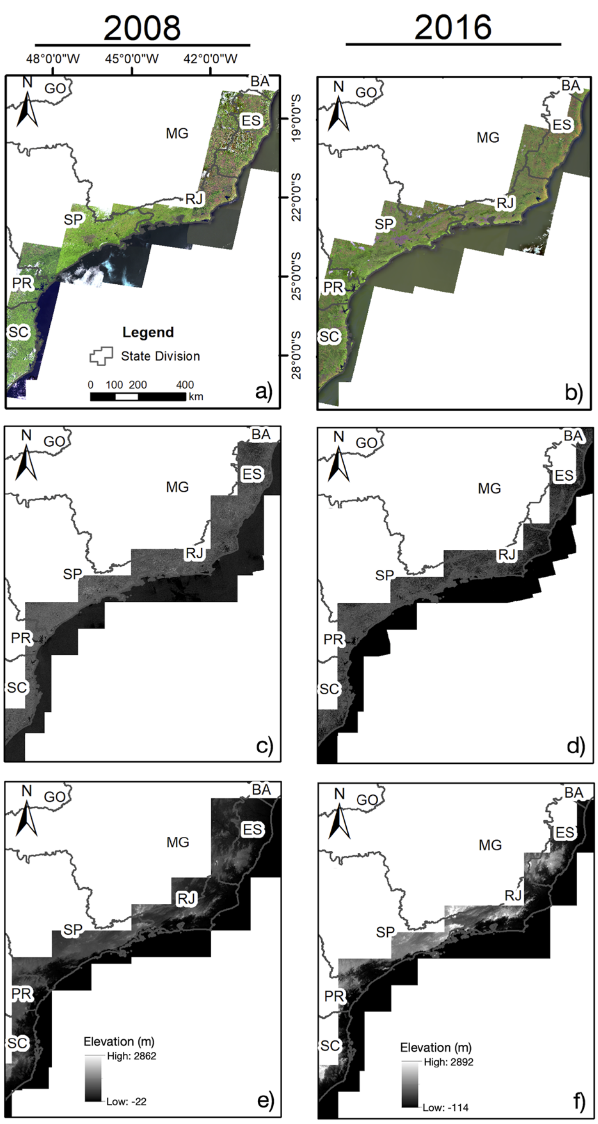

Figure 2. Example of a set of space-borne images used to map mangroves. a) Landsat-5 TM image in color composite 5R4G3B; b) Landsat-8 OLI in color composite 6R5G4B; c) 2008 and d) 2016 ALOS PALSAR monochromatic L-band in HH-polarization images; e) 2000 SRTM digital elevation model; and f) 2014 ALOS PALSAR digital elevation model.

Segmentation level 2 was established below level 1, i.e., level 2 image objects were included in the level 1 image objects to increase the level of detail of the segmentation. The optical sensor images were assigned the highest weights in level 2. The main objective of the level 2 segmentation was to separate the mangrove vegetation from upland vegetation. Radar images were used to classify mangroves below clouds, albeit with lower weights than the other images. Hence, 67.30 km² of mangrove areas under clouds were mapped. This represents approximately 8% of the total area mapped in 2008. In 2016, there were no clouds in the study site. Figure 3 illustrates the differences between the segmentation levels.

In level 3, the classification was refined using the same scale and heterogeneity parameters as level 2. Images of the mangrove class were grouped separately. Border relations between the mangrove and upland classes were used to remove some incorrect mangrove classifications resulting from confusion of the spectral responses of the targets. Thus, polygons classified as mangrove in the continental domain were reclassified as upland class. The expressions used in the classifications and modifications are shown in Table II.

First, the water bodies and continent (coastal plain and upland) classes were classified. The classification parameters were defined mainly based on the backscatter values (in decibels-dB) of the SAR data, as represented by "Expression 1", and were essential to define the coastline (Table II). The mangrove class was classified next. The parameters were chosen based on the mean reflectance of the red, near-infrared and mid-infrared Landsat-5 TM spectral bands (Mean B3, B5 and B7, respectively) and the Landsat-8 OLI bands 4, 5 and 6 (red, near-infrared and shortwave infrared, respectively) using "Expression 2" (Table II). Other expressions

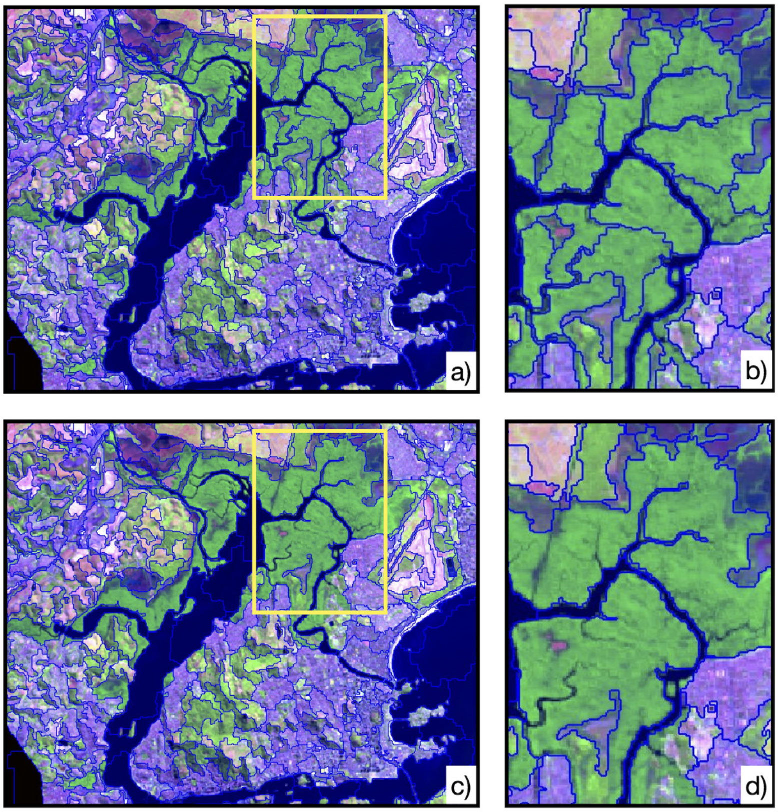

Figure 3. **Multiresolution segmentation. a) and b) Segmentation level 2. c) and d) Segmentation level 1. Observe that segmentation level 1 presents larger and fewer objects in comparison to level 2. Note in detail (yellow box in figure a and c) differences between segmentation levels (figure b and d).**

Table II. **Expressions used to classify mangrove area.**

Description	(2008)	(2016)
Expression 1	10 x log (Mean HV)	10 x log (Mean HV)
Expression 2	[(Mean B5 – Mean B3)/(Mean B5 + Mean B3)] + Mean B7	[(Mean B5 – Mean B4)/(Mean B5 + Mean B4)] + Mean B6
Expression 3	Mean HV/Mean DEM	Mean HV/Mean DEM
Expression 4	10 x log (Mean HV)/DEM	10 x log (Mean HV)/DEM

were also used to optimize the mangrove classification process for 2008 and 2016 (Table II). “Expression 3” consists of an average ratio between SAR and DEM data and was essential in the mapping mangroves below clouds, as was “Expression 4”. DEM was also used alone as an alternative to limit the occurrence of mangroves using the forest canopy height. Figure 4 shows the process tree used to classify the three main classes mentioned above and the parameters used for each segmentation level.

The mangroves were classified following the sequence detailed in Figure 4. Initially, the water bodies (rivers, lakes, and ocean) and the continent were classified to define the coastline. The mangroves were then classified by combining the reflectance of the red and infrared bands with the backscatter of the PALSAR images and the elevation of the SRTM and ALSO DEM. The Landsat scenes provided the spectral interval to characterize the mangrove, the PALSAR images were used to identify the forest cover, and the DEM enabled separation of the mangrove vegetation by canopy height.

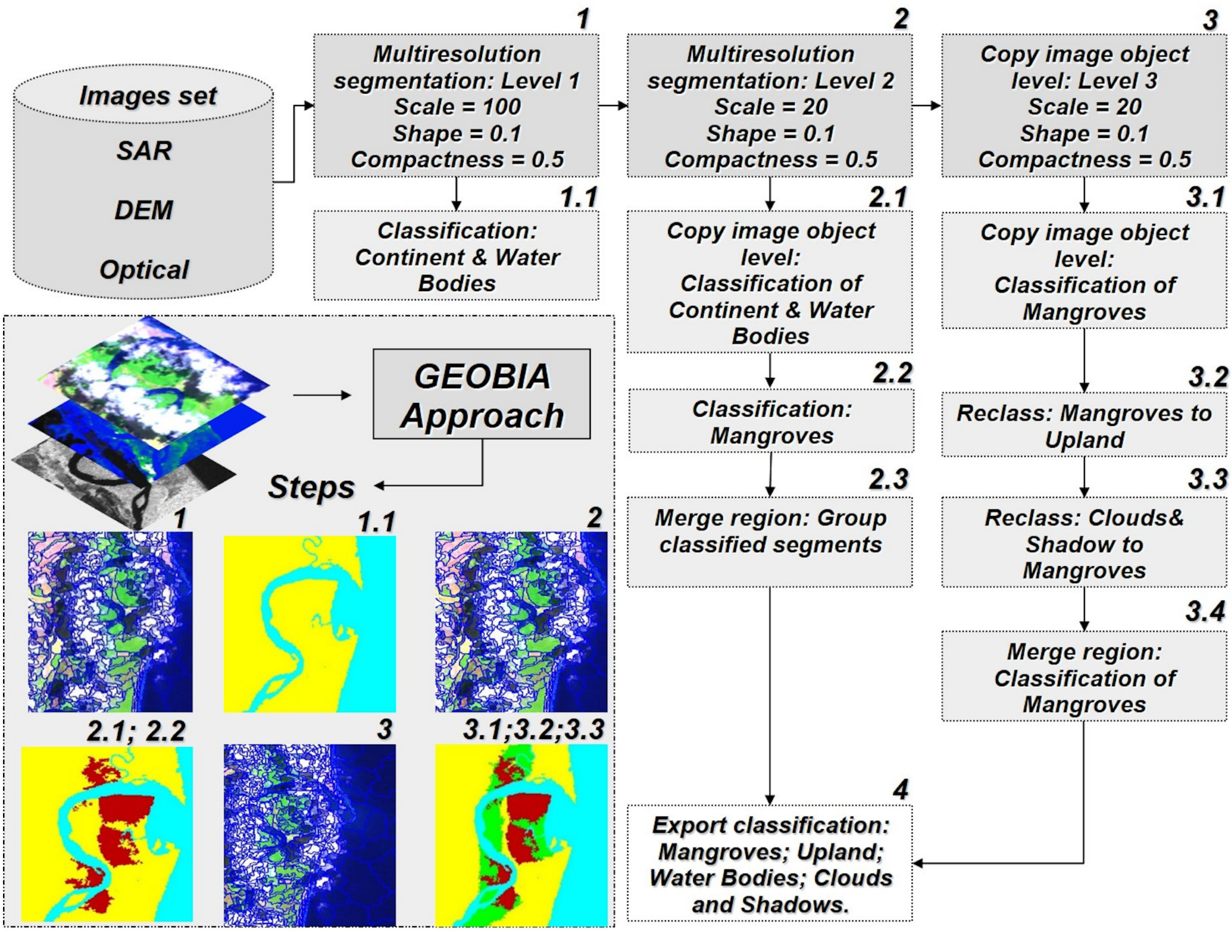

Figure 4. Flowchart showing processing steps for mangrove classification: SAR, optical and DEM images were subjected to three segmentation levels, and mangrove classification was obtained after combination of segmentation levels 2 and 3.

Object-oriented change detection

An object-oriented change detection analysis was adapted from the methodology proposed by Nascimento Jr et al. (2013) The mangrove 2008 and mangrove 2016 classes were initially generated. Arithmetic operations were used to generate the classes of gain, loss and no change for the mangrove area (Schlosser & Pfirman 2012). The gain class represented areas that were present in the mangrove 2016 class but not the mangrove 2008 class. The loss class represented areas that were not present in the mangrove 2016 class; that is, areas that were only classified in the mangrove 2008 class. Finally, the no change class represented unchanged areas, i.e. those areas that remained constant for the two classifications. Figure 5 is a flowchart summarizing all the change detection stages.

Evaluation of object-oriented classification.

The classification was evaluated using a collection of control points on high-resolution images of the Google Earth Pro platform. These points were selected very close to the limits of what were believed to be mangrove areas or locations likely to be confused with other classes. Thus, both the segmentation and classification were evaluated for areas with close separability thresholds. A total of 600 control points were collected, of which 300 were chosen

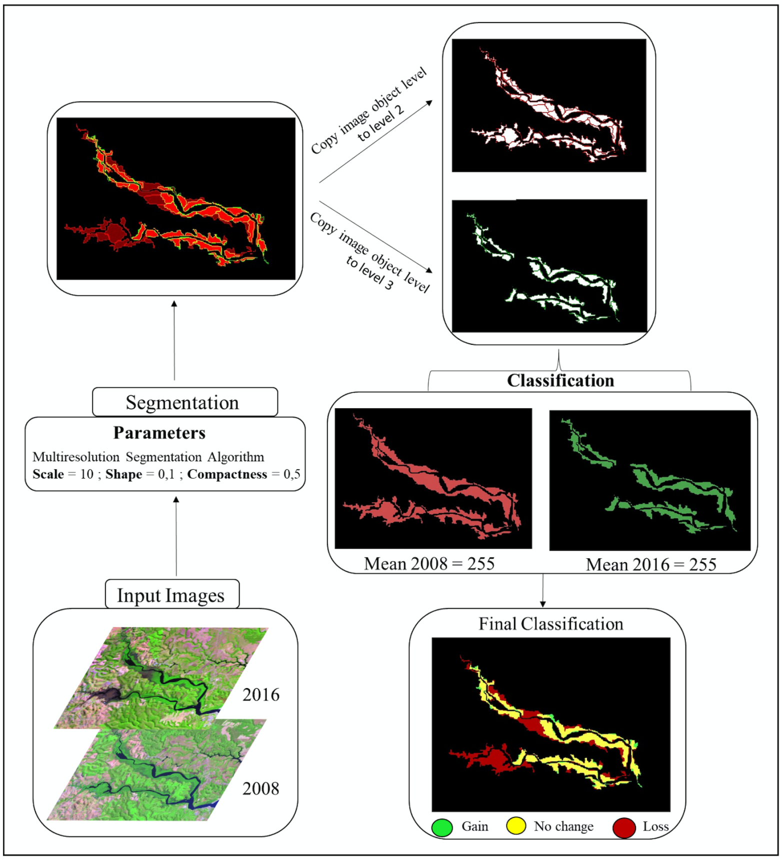

Figure 5. Example of change detection process using detail of area in Espírito Santo state, near the mouth of the Piraquê-Açu river. First: Input images of Landsat mosaics 2008 and 2016. Second: Segmentation of Landsat mosaics 2008 and 2016. Third: Classification for respective years from geographical object-based image analysis. Finally, object-oriented change detection analysis was performed to identify areas of gain, loss, and no change of mangrove forests.

in mangrove areas and 300 were in regions that could be confused with mangroves.

The mangrove classification using multisource remote sensors was validated using confusion matrices and the following classical indices: the Kappa index (Congalton 1991), user's and producer's accuracies (Story & Congalton 1986), the Kappa coefficient per class (Congalton & Green 2019) and the Tau index (Ma & Redmond 1995). Disagreements were also evaluated (Pontius Jr & Millones 2011). For this purpose, allocation (AD) and quantity disagreements (QD) provided measures of discordance due to the imperfect spatial allocation of class polygons and due to the incorrect extent of classes, respectively. AD is important to change detection as spatial mismatches during map comparisons may result with the detection of false transitions. While QD is important when the aim is to compute areal differences in classes among maps (Pontius Jr & Millones 2011).

For the change detection analysis, 1000 control points were distributed between the gain, loss and no change classes, which were also calculated using the indices cited above and the area estimates (Olofsson et al. 2014). The objective of this analysis followed best practices for accuracy assessment of the change classification and estimation of area of change in terms of a classification error matrix. The error matrix was used to cross-tabulate the land change class labels allocated by the classification against the reference GCPs collected at sample sites. Accuracy parameters derived from a sample error matrix included overall accuracy, user and producer accuracy of each class (Olofsson et al. 2014).

RESULTS

GEOBIA was used with multisensor data to map the mangroves in the coastal region of South and Southeast Brazil. Images and detailed maps are shown in Figure 6. The coastal zone of the study area contained 823.03 km² of mangrove forests in 2008, which decreased to 789.00 km² in 2016. This reduction in the mangrove area of approximately 34 km² is equivalent to a 4.1% loss.

Throughout the study period, a loss of mangrove area was found for almost all coastal states, except RJ, which was characterized by a 3.6% expansion of mangrove areas. The highest mangrove area losses were recorded for ES (~20%), followed by SC (~13%), SP (~3%) and PR (0.45%).

Classification accuracy

For 2008, 278 or 92.67% of the 300 points collected in the mangrove area were correctly classified, whereas 22 points or 7.33% did not match the sampled points. The classification accuracy for mangrove areas in 2016 was the same as for 2008, i.e. 278 or 92.67% of the 300 collected points were correctly classified.

For each year, 300 points were also sampled for the "others" class, of which 274 or 93.6% were classified correctly in 2008, and 26 points or 8.6% did not match the sampled points. The accuracy of the "others" class was higher for 2016 than for 2008: 281 or 93.7% of the 300 collected points were classified correctly for 2016, whereas 19 points or 6.3% did not match the classification.

Several indices were also used to assess the classification accuracy. The following values were obtained for 2008: an overall Kappa index of 0.84; the Kappa index per class reached 0.85 for the mangrove class and 0.82 for the "others" class; an overall accuracy of 92% and a Tau index of 0.84 (Table III). The following values were obtained for 2016: an overall Kappa index

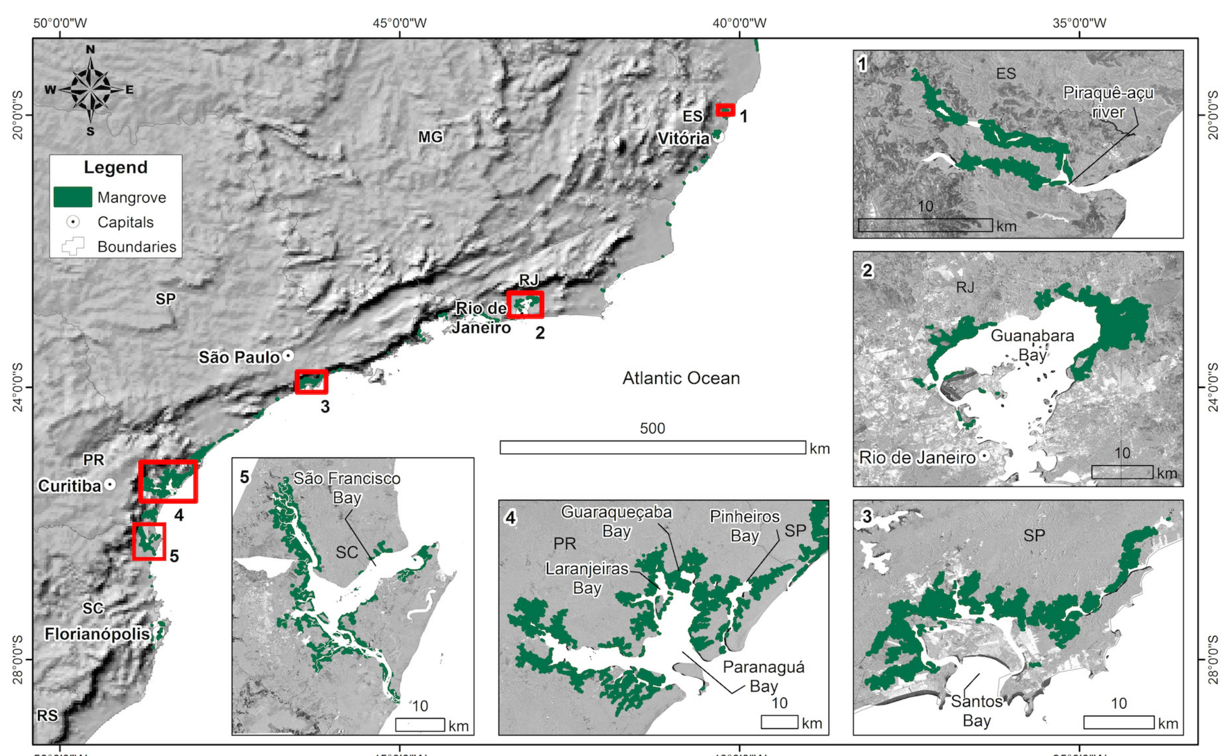

Figure 6. Detailed map of mangrove areas for most representative regions of investigated states in 2016.

of 0.86; a Kappa index per class of 0.85 for the mangrove class and 0.87 for the “others” class; a 93% overall accuracy and a Tau index of 0.86 (Table III).

Geographical object-oriented change detection

The change detection accuracy was evaluated using the random and stratified distributions of 1000 control points. The overall accuracy was 86.50%. Of 13.50% disagreements (Pontius Jr & Millones 2011), 5.60% were quantity disagreements, and 7.90% were allocation disagreements. The largest quantity disagreements (5.60%) were observed for the no change mangrove class, and the largest allocation disagreements were related to the gain mangrove class (5.80%).

The area estimates were adjusted using the methodology of Olofsson et al. (2014). There were more losses than initially quantified, resulting in fewer unchanged areas than initially estimated. The quantity of gains was almost constant. Table IV summarizes the main data obtained from the confusion matrix.

The change detection analysis was used to identify areas of expansion, reduction and no change in mangrove vegetation. The unchanged mangrove areas represented approximately 80% of the study area, for which the largest percentage (~84%) corresponded to RJ, followed by PR (~82%) and SP (80%). There was a 20.90% loss and a 16.80% gain in mangrove areas over the entire period of study. An analysis of the balance between the total gains and losses of the mangrove areas showed that all states had

Table III. Classification confusion matrix for 2008 (A) and 2016 (B).

A) 2008					
	Mangrove	**Others**	**Total**	**User’s Accuracy**	**Commission Error**
Mangrove	278	22	304	91.4	8.5
Others	26	274	296	92.5	7.4
Total	300	300	600		
Omission error	7.33	8.6			
Producer’s Accuracy	92.6	91.3			
Kappa per class	0.85	0.82			
Overall accuracy = 0.92		Kappa index = 0.84			Tau index = 0.84
B) 2016					
	Mangrove	Others	Total	User’s Accuracy	Commission Error
Mangrove	278	22	297	93.6	6.3
Others	19	281	303	92.7	7.2
Total	300	300	600		
Omission error	7.33	6.3			
Producer’s Accuracy	92.6	93.6			
Kappa per class	0.85	0.87			
Overall accuracy = 0.92			Kappa index = 0.84		Tau index = 0.84

higher losses of mangrove areas than gains over the period of study, except for RJ, which exhibited more gains in mangrove areas than losses. Figure 7 is a graphical illustration of the balance between losses and gains of mangrove areas by state.

Considerable changes were observed near the Piraquê-açu River in ES. Guanabara Bay was representative of gain and loss of mangrove areas in RJ. The most significant changes in SP occurred in the vicinity of Santos Bay. Changes in PR mainly occurred in the Paranaguá Estuarine Complex - CEPII, which comprises four bays (Paranaguá, Pinheiros, Guaraqueçaba and Laranjeiras) with extensive mangrove areas. Most of the mangrove areas in SC are found in the São Francisco Bay or Babitonga. Figure 8 is a change detection map for the entire study area, wherein the areas mentioned above are highlighted.

DISCUSSION

Mangrove extent in South and Southeast Brazil

The analysis of remote sensing images to quantify the mangrove area in the coastal zone of South and Southeast Brazil is important for conservation. The mangrove forest area in South and Southeast Brazil was estimated at 823.03 and 789.00 km^2 for 2008 and 2016, respectively, in this study. Different methods have previously been used to estimate the mangrove area: for example, the SOS *Mata Atlântica* (Atlantic Forest) project (SOS Mata Atlântica 2018) and the Mapbiomas project (2019), conducted by Diniz et al. (2019), quantified the mangrove area for South and Southeast Brazil at 892.9 km^2 and 636.02 km^2, respectively, for 2008 and at 953.8 km^2 and 615.14 km^2, respectively, for 2016. Figure 9 shows the mangrove areas estimated by different authors for each of the coastal states of South and Southeast Brazil (Diniz et al. 2019, SOS Mata Atlântica 2009, 2018).

The estimates obtained in the present study are generally similar to those obtained by the Mapbiomas project, given the similar nature of the data analysed. That is, Landsat images, with 30-m spatial resolution, were used to map mangrove forests. ALOS PALSAR images were also used in this study to minimize the effect of cloud cover that was around 8% in 2008, whereas a series of cloud-free images (Diniz et al. 2019) were used in the Mapbiomas project. In both studies, a loss of mangrove areas was observed, with the exception of RJ, for which there was a mangrove gain. Relatively larger areas were estimated by the Atlântica project (2009, 2018), because the mangrove ecosystem was mapped as a whole, considering both mangrove forests and associated hypersaline fields, locally known as “apicum”. Our estimate can be considered more accurate than previous estimates because of the inclusion of ALOS PALSAR images, with a 10-m spatial resolution, which are associated with Landsat images and classified using GEOBIA instead of isolated pixels.

Table IV. Summary of data obtained from confusion matrix for change detection. Loss, gain and no change were calculated from methodological approach proposed by Olofsson et al. (2014). Overall accuracy (OA), overall disagreement (OD), quantity disagreement (QD), and allocation disagreement (AD) were estimated from Pontius Jr & Millones’ (2011).

CLASS	Calculated data (km²)	Data adjusted following (km²) by Olofsson *et al.* (2014)
LOSS	172.24	221 ± 19
GAIN	138.21	132 ± 17
NO CHANGE	650.79	618 ± 20

OA = 86.50	**OD =** 13.50	**QD =** 5.60	**AD =** 7.90

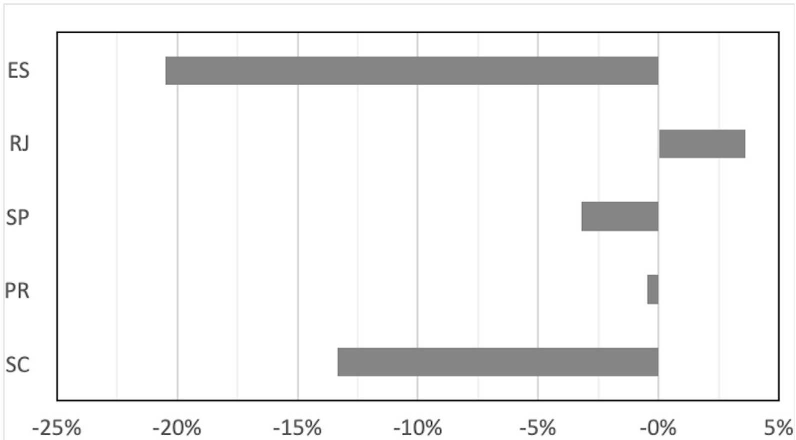

Figure 7. Balance of gain and loss of mangrove areas for each state from 2008 to 2016.

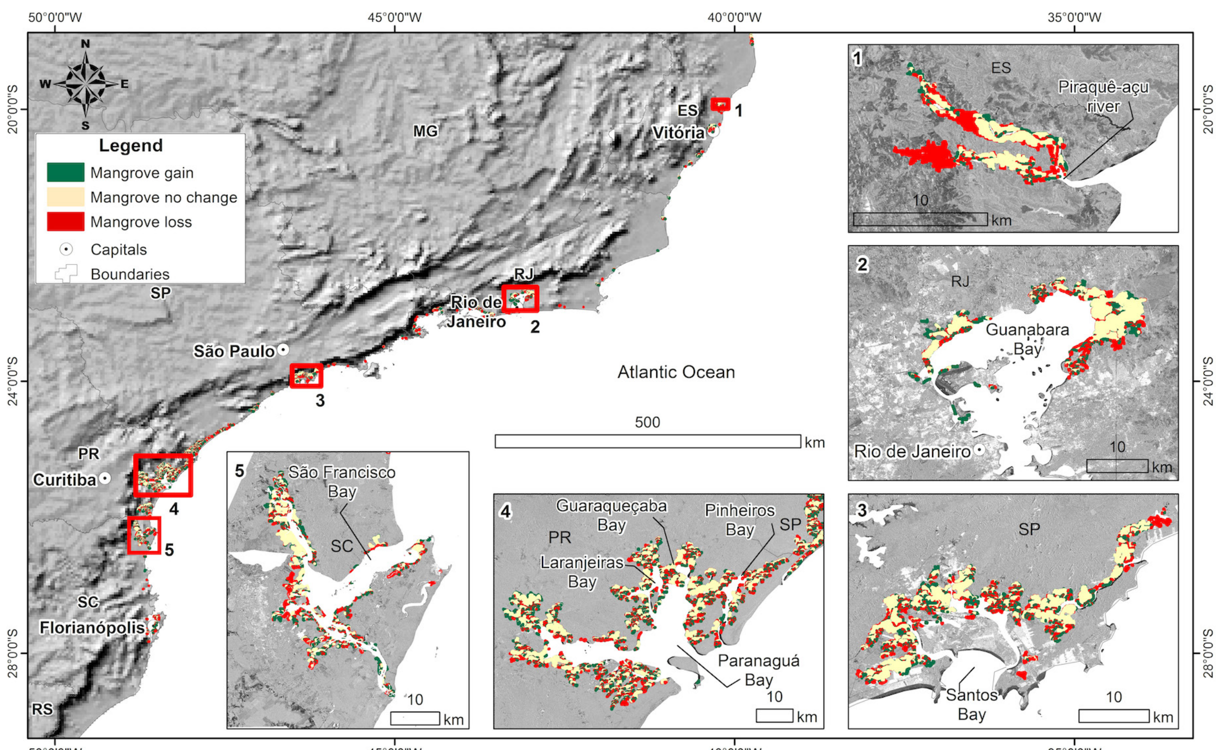

Figure 8. Change detection map for study area: regions with most significant changes for each state are demarcated by red boxes.

Mangrove losses in South and Southeast Brazil and elsewhere

Over 56% of the Brazilian population reside in South and Southeast Brazil (IBGE 2011). These regions have the highest demographic densities, ranging from 49 to 87 inhabitants per km^2, but surprisingly lost only 4% of their mangrove area over the last decade. Furthermore, the fringed mangroves of the southeast and south of Brazil are bounded by highland areas ("Serra do Mar") and are the ones most threatened by sea-level rise (Souza-Filho et al. 2023). The loss of mangrove area is mainly related to processes of occupation of the coastal zone as observed in Piraquê-Açu river, Espírito Santo State (Figure 8) due to impact of upland use in the adjacent

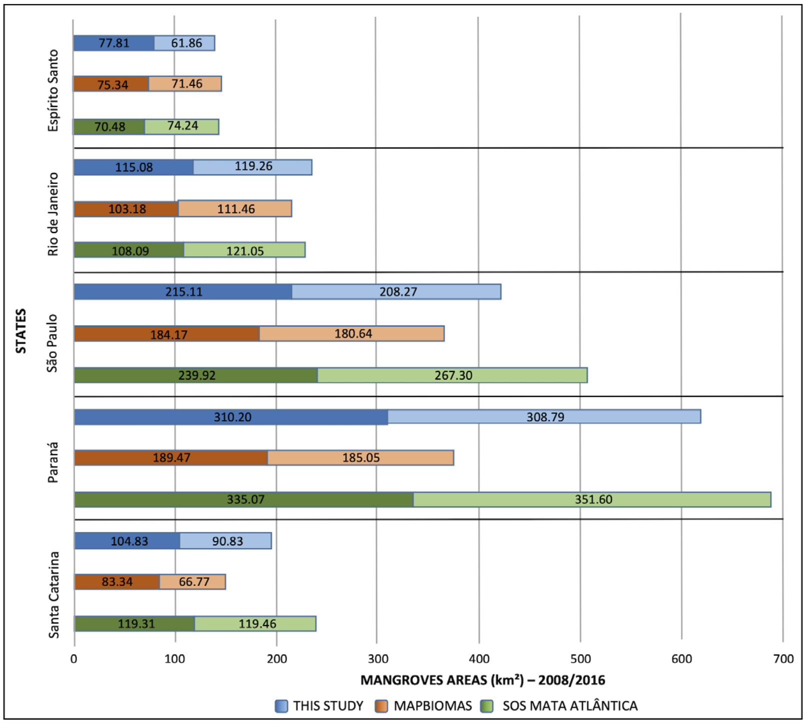

Figure 9. Estimates of mangrove area by different authors for the coastal states of South and Southeast Brazil (MAPBIOMAS - Diniz et al. 2019, SOS Mata Atlântica 2009, 2018).

mangrove and Florianópolis Island (Trindade 2009), whereas expansion is associated with the progradation of mudflats subsequently colonized by mangrove vegetation in protected areas within coastal bays, such as Santos and Guanabara bays (Figure 8), where mangrove forest presents higher structural development (Cavalcanti et al. 2009)

Comparing this dynamic with other regions of the country shows that the highest loss of mangrove area in Brazil is in the South and Southeast, because the mangrove area remained practically stable over the period analysed in the Northeast region (MapBiomas 2018), and there was an increase of approximately 10% in the North (Nascimento Jr et al. 2013). However, we found that the mangroves of South and Southeast Brazil (the most densely populated region of Brazil) are still well preserved in comparison to other developing regions with high population densities, such as China, the Philippines and Vietnam. For example, China has lost 48% of its mangrove area over the last 50 years (Jia et al. 2018), whereas the Philippines (Primavera 2000) and Vietnam (Valiela et al. 2001) lost 73% and 62%, respectively. Furthermore, in response to global changes associated to warming process, Soares et al. (2012) expect that mangrove forest will expand southward of their present latitudinal limit at Laguna, Santa Catarina State.

Brazilian mangroves have been successfully conserved in response to public policies, that is, mangrove areas have been permanently protected since the publication of the Brazilian Constitution of 1988. In addition, a series of sustainable-use conservation units, including extractive and restricted-use reserves, such as national parks and biological reserves (Gerhardinger et al. 2009, Tenório et al. 2015), were created along the Brazilian coast, making it difficult to annex mangrove areas for different use purposes.

Major drivers of mangrove changes in the study site are related to port activities (Ferreira & Lacerda 2016), urbanization (Lacerda et al.

2019, Trindade 2009), climate changes (Godoy & Lacerda 2015, Soares et al. 2012) and the new Brazilian Forest Code - (Brasil 2012, Borges et al. 2017). Due to lack of proper evaluation of mangrove functioning along the Brazilian coast and environmental inconsistencies of the new Brazilian Forest Code that excluded salt flats from mangrove protection areas, anthropogenic drivers have the potential to increase threats and reduce the effectiveness of conservation of this important ecosystem (Oliveira-Filho et al. 2016). At least, an annual assessment of mangrove extension has been carried out from MapBiomas project (Souza et al. 2020, Diniz et al. 2019), hence will be possible to assess the status and sustainable use of mangrove forest and salt flats along the Brazilian coast to break negative anthropogenic impacts on mangroves. Restoration efforts need to be increased to minimized losses and expand the use of natural services given by mangrove forests (Ferreira & Lacerda 2016).

CONCLUSIONS

Satisfactory results were obtained by using optical and radar remote sensing data in conjunction with GEOBIA techniques to map mangrove forest areas in South and Southeast Brazil. This alternative mapping scheme exploits the advantages of different sensor types, irrespective of their characteristics. There has been an overall 4% reduction in the mangrove areas of South and Southeast Brazil over the last decade. This reduction is reflected in all states except in Rio de Janeiro. The mangrove area loss of 4% is considered low in the most densely populated region of Brazil. Hence, we have an important opportunity to tell success stories that have helped protect mangroves, making then an important and positive case study for the conservation optimism movement for now (Friess et al. 2020).

The results obtained in this study can be used as a reference for future studies and to monitor the development and dynamics of mangroves to evaluate the main natural and anthropogenic factors affecting change in the coastal landscape of South and Southeast Brazil.

Acknowledgments

The authors acknowledge financial support from the Coordenação de Aperfeiçoamento de Pessoal de Nível Superior (CAPES-Brazil) and the Conselho Nacional de Desenvolvimento Científico e Tecnológico (CNPq- Proc. # 310283/2019-1).

REFERENCES

ALONGI DM. 2008. Mangrove forests: resilience, protection from tsunamis, and responses to global climate change. Estuar Coast Shelf Sci 76: 1-13.

BORGES R, FERREIRA AC & LACERDA LD. 2017. Systematic Planning and Ecosystem-Based Management as Strategies to Reconcile Mangrove Conservation with Resource Use. Front Mar Sci 4.

BRASIL L. 2012. Código Florestal Brasileiro - Lei Nº 12.651, de 25 de Maio de 2012 [Online]. Brasília - DF: Congresso Nacional. Available: http://www.planalto.gov.br/ccivil_03/_ato2011-2014/2012/lei/l12651.htm.

CAVALCANTI V, SOARES M, ESTRADA G & CHAVES FJJOCR. 2009. Evaluating mangrove conservation through the analysis of forest structure data. 390-394.

CONGALTON RG. 1991. A review of assessing the accuracy of classifications of remotely sensed data. Remote Sens Environ 37: 35-46.

CONGALTON RG & GREEN K 2019. Assessing the accuracy of remotely sensed data: principles and practices. CRC press.

DINIZ C, CORTINHAS L, NERINO G, RODRIGUES J, SADECK L, ADAMI M & SOUZA-FILHO PWM. 2019. Brazilian Mangrove Status: Three Decades of Satellite Data Analysis. Remote Sens 11: 808.

FERREIRA AC & LACERDA LD. 2016. Degradation and conservation of Brazilian mangroves, status and perspectives. Ocean Coast Manag 125: 38-46.

FRIESS DA ET AL. 2020. Mangroves give cause for conservation optimism, for now. Curr Biol 30: R153-R154.

GERHARDINGER LC, GODOY EA & JONES PJ. 2009. Local ecological knowledge and the management of marine protected areas in Brazil. Ocean Coast Manag 52: 154-165.

GIRI C, OCHIENG E, TIESZEN LL, ZHU Z, SINGH A, LOVELAND T, MASEK J & DUKE N. 2011. Status and distribution of mangrove forests of the world using earth observation satellite data. Glob Ecol Biogeogr 20: 154-159.

GLASER M. 2003. Interrelations between mangrove ecosystem, local economy and social sustainability in Caeté Estuary, North Brazil. Wetl Ecol Manag 11: 265-272.

GODOY MD & LACERDA LD. 2015. Mangroves Response to Climate Change: A Review of Recent Findings on Mangrove Extension and Distribution. An Acad Bras Cienc 87: 651-667.

GREEN E, CLARK C, MUMBY P, EDWARDS A & ELLIS A. 1998. Remote sensing techniques for mangrove mapping. Int J Remote Sens 19: 935-956.

HERZ R. 1991. Manguezais do Brasil. São Paulo: Universidade de São Paulo.

IBGE. 2011. Censo Demográfico 2010: Sinopse do Censo 2010. IBGE Rio de Janeiro.

JIA M, WANG Z, ZHANG Y, MAO D & WANG C. 2018. Monitoring loss and recovery of mangrove forests during 42 years: The achievements of mangrove conservation in China. Int J Appl Earth Obs Geoinf 73: 535-545.

KAMAL M, PHINN S & JOHANSEN K. 2015. Object-Based Approach for Multi-Scale Mangrove Composition Mapping Using Multi-Resolution Image Datasets. Remote Sens 7: 4753-4783.

KARTIKEYAN B, SARKAR A & MAJUMDER KL. 1998. A segmentation approach to classification of remote sensing imagery. Int J Remote Sens 19: 1695-1709.

LACERDA LD, BORGES R & FERREIRA AC. 2019. Neotropical mangroves: Conservation and sustainable use in a scenario of global climate change. Aquatic Conservation: Marine and Freshwater Ecosystems 29: 1347-1364.

MA Z & REDMOND RL. 1995. Tau coefficients for accuracy assessment of classification of remote sensing data. Photogramm Eng Remote Sens 61: 435-439.

MAPBIOMAS P. 2018. Coleção 2 da Série Anual de Mapas de Cobertura e Uso de Solo do Brasil. mapbiomas org> acessado em 11.

NASCIMENTO JR WR, SOUZA-FILHO PWM, PROISY C, LUCAS RM & ROSENQVIST A. 2013. Mapping changes in the largest continuous Amazonian mangrove belt using object-based classification of multisensor satellite imagery. Estuar Coast Shelf Sci 117: 83-93.

OLIVEIRA-FILHO RRD, ROVAI AS, MENGHINI RP, COELHO JÚNIOR C, SCHAEFFER NOVELLI Y & CINTRÓN G. 2016. On the impact of the Brazilian Forest Code on mangroves: A comment to Ferreira and Lacerda (2016). Ocean Coastal Manag 132: 36-37.

OLOFSSON P, FOODY GM, HEROLD M, STEHMAN SV, WOODCOCK CE & WULDER MA. 2014. Good practices for estimating area and assessing accuracy of land change. Remote Sens Environ 148: 42-57.

PEREIRA EA. 2015. A dinâmica dos manguezais no nordeste do Brasil: Uma abordagem a partir de dados de sensores remoto e SIG. Phd Thesis, Programa de Pós-Graduação em Geologia e Geoquímica, Universidade Federal do Pará.

PONTIUS JR RG & MILLONES M. 2011. Death to Kappa: birth of quantity disagreement and allocation disagreement for accuracy assessment. Int J Remote Sens 32: 4407-4429.

PRIMAVERA JH. 2000. Development and conservation of Philippine mangroves: institutional issues. Ecol Econ 35: 91-106.

ROSENQVIST A, SHIMADA M, ITO N & WATANABE M. 2007. ALOS PALSAR: A Pathfinder Mission for Global-Scale Monitoring of the Environment. IEEE Trans Geosci Remote Sens 45: 3307-3316.

SANTOS DC. 2012. Reconhecimento e mapeamento de gêneros de mangue a partir de dados espectrorradiométricos e imagens ikonos na Ilha de Marajó-Pa.

SCHLOSSER P & PFIRMAN S. 2012. Earth science for sustainability. Nature Geosci 5: 587-588.

SOARES MLG, ESTRADA GCD, FERNANDEZ V & TOGNELLA MMP. 2012. Southern limit of the Western South Atlantic mangroves: Assessment of the potential effects of global warming from a biogeographical perspective. Estuar Coast Shelf Sci 101: 44-53.

SOS MATA ATLÂNTICA. 2009. Atlas dos Remanescentes Florestais da Mata Atlântica–Período 2005-2008. Relatório Técnico São Paulo[acessed in April 4th, 2019] Available in: https://wwwsosmaorgbr/projeto/atlas-da-mata-atlantica/dados-mais-recentes.

SOS MATA ATLÂNTICA. 2018. Atlas dos remanescentes florestais da Mata Atlântica: período 2016-2017. Relatório Técnico São Paulo[acessed in April 4th, 2019] Available in: https://wwwsosmaorgbr/projeto/atlas-da-mata-atlantica/dados-mais-recentes.

SOUZA CM ET AL. 2020. Reconstructing Three Decades of Land Use and Land Cover Changes in Brazilian Biomes with Landsat Archive and Earth Engine. Remote Sens 12.

SOUZA-FILHO PWM. 2005. Costa de manguezais de macromaré da Amazônia: cenários morfológicos, mapeamento e quantificação de áreas usando dados de senores remotos. Rev Bras Geofís 23: 427-435.

SOUZA-FILHO PWM, DINIZ CG, E SOUZA-NETO PWM, LOPES JPN, DA NASCIMENTO JÚNIOR WR, CORTINHAS L, ASP NE, FERNANDES MEB & DOMINGUEZ JML 2023. Mangrove Swamps of Brazil: Current Status and Impact of Sea-Level Changes. In: DOMINGUEZ, JML, KIKUCHI, RKPD, FILHO, MCDA, SCHWAMBORN R AND VITAL H (Eds) Tropical Marine Environments of Brazil: Spatio-Temporal Heterogeneities and Responses to Climate Changes, Cham: Springer International Publishing, p. 45-74.

SOUZA-FILHO PWM & PARADELLA WR. 2002. Recognition of the main geobotanical features along the Bragança mangrove coast (Brazilian Amazon Region) from Landsat TM and RADARSAT-1 data. Wetl Ecol Manag 10: 123-132.

SOUZA-FILHO PWM & PARADELLA WR. 2005. Use of RADARSAT-1 fine mode and Landsat-5 TM selective principal component analysis for geomorphological mapping in a macrotidal mangrove coast in the Amazon region. Can J Remote Sens 31: 214-224.

STORY M & CONGALTON RG. 1986. Accuracy assessment: a user's perspective. Photogramm Eng Remote Sens 52: 397-399.

TENÓRIO GS, SOUZA-FILHO PWM, RAMOS EM & ALVES PJO. 2015. Mangrove shrimp farm mapping and productivity on the Brazilian Amazon coast: Environmental and economic reasons for coastal conservation. Ocean Coast Manag 104: 65-77.

TERCHUNIAN A, KLEMAS V, SEGOVIA A, ALVAREZ A, VASCONEZ B & GUERRERO L. 1986. Mangrove mapping in Ecuador: The impact of shrimp pond construction. Environ Manag 10: 345-350.

TRINDADE L. 2009. Os manguezais da Ilha de Santa Catarina frente à antropização da paisagem. Dissertação de Mestrado, Programa de Pós-Graduação em Arquitetura e Urbanismo, Universidade Federal de Santa Catarina. (Unpublished).

USGS. 2012. Landsat Data Continuity Mission (LDCM) Level 1 (L1) Data Format Control Book (DFCB). Sioux Falls, South Dakota: U.S. Geological Survey, Department of the Interior, p. 21.

VALIELA I, BOWEN JL & YORK JK. 2001. Mangrove Forests: One of the World's Threatened Major Tropical Environments: At least 35% of the area of mangrove forests has been lost in the past two decades, losses that exceed those for tropical rain forests and coral reefs, two other well-known threatened environments. Bioscience 51: 807-815.

How to cite

LOPES JPN, NASCIMENTO JR WR, DINIZ CG & SOUZA-FILHO PWM. 2023. Mangrove changes over the past decade in South and Southeast Brazil using spaceborne optical and SAR imagery. An Acad Bras Cienc 95: e20201533. DOI 10.1590/0001-3765202320201533.

Manuscript received on September 29, 2020; accepted for publication on March 2, 2021

JOÃO PAULO N. LOPES[1,2]
https://orcid.org/0000-0001-7872-447X

WILSON R. NASCIMENTO JR[2]
https://orcid.org/0000-0002-0720-4933

CESAR G. DINIZ[3]
https://orcid.org/0000-0001-7718-0992

PEDRO WALFIR M. SOUZA-FILHO[1,2]
https://orcid.org/0000-0003-0252-808X

[1]Universidade Federal do Pará, Instituto de Geociências, Rua Augusto Correa, 1, 66075-110 Belém, PA, Brazil

[2]Instituto Tecnológico Vale, Rua Boaventura da Silva, 955, 66055-090 Belém, PA, Brazil

[3]Solved – Soluções em Geoinformação, Parque de Ciência e Tecnologia Guamá, Avenida Perimetral da Ciência, Km 01, 66075-750 Belém, PA, Brazil

Correspondence to: **Pedro Walfir M. Souza-Filho**
E-mail: pedro.martins.souza@itv.org

Author contributions

P.W.M.S.F, J.P.N.L and W.R.N.Jr made substantive intellectual contributions to the manuscript. J.P.N.L. participated in the execution of the research and in the planning, analysis and preparation of the manuscript; W.R.N.Jr and PWM Souza-Filho supervised the project, participated in the execution of the research and in the planning, analysis and preparation of the manuscript; J.P.N.L., W.R.N.Jr and C.G.D. contributed to the digital processing of images and participated in the analysis of the results.